AGU PUBLICATIONS

JGR

Journal of Geophysical Research: Atmospheres

RESEARCH ARTICLE

10.1002/2013JD021114

Key Points:
- Nonfossil carbon concentrations in Pasadena are constant throughout the day
- Fossil afternoon increase after arrival of the western Los Angeles basin plume
- Fossil increase is mainly due to fresh SOA formed in the LA basin plume

Supporting Information:
- Readme
- Figures S1–S7 and Tables S1 and S2

Correspondence to:
A. S. H. Prévôt,
andre.prevot@psi.ch

Citation:
Zotter, P., et al. (2014), Diurnal cycle of fossil and nonfossil carbon using radiocarbon analyses during CalNex, *J. Geophys. Res. Atmos.*, *119*, 6818–6835, doi:10.1002/2013JD021114.

Received 30 OCT 2013
Accepted 17 APR 2014
Accepted article online 23 APR 2014
Published online 3 JUN 2014

Diurnal cycle of fossil and nonfossil carbon using radiocarbon analyses during CalNex

Peter Zotter[1], Imad El-Haddad[1], Yanlin Zhang[1,2,3], Patrick L. Hayes[4,5], Xiaolu Zhang[6,7], Ying-Hsuan Lin[8], Lukas Wacker[9], Jürgen Schnelle-Kreis[10], Gülcin Abbaszade[10], Ralf Zimmermann[10,11], Jason D. Surratt[8], Rodney Weber[6], José L. Jimenez[4], Sönke Szidat[2,3], Urs Baltensperger[1], and André S. H. Prévôt[1]

[1]Laboratory of Atmospheric Chemistry, Paul Scherrer Institute, Villigen, Switzerland, [2]Department of Chemistry and Biochemistry, University of Bern, Bern, Switzerland, [3]Oeschger Centre for Climate Change Research, University of Bern, Bern, Switzerland, [4]Department of Chemistry and CIRES, University of Colorado, Boulder, Colorado, USA, [5]Now at Département de Chimie, Université de Montréal, Montréal, Quebec, Canada, [6]School of Earth and Atmospheric Sciences, Georgia Institute of Technology, Atlanta, Georgia, USA, [7]Now at Department of Civil and Environmental Engineering, University of California Davis, Davis, California, USA, [8]Department of Environmental Sciences and Engineering, Gillings School of Global Public Health, University of North Carolina at Chapel Hill, Chapel Hill, North Carolina, USA, [9]Laboratory of Ion Beam Physics, ETH Hönggerberg, Zürich, Switzerland, [10]Joint Mass Spectrometry Centre, Cooperation Group Comprehensive Molecular Analytics, Helmholtz Zentrum München, German Research Center for Environmental Health (GmbH), Neuherberg, Germany, [11]Joint Mass Spectrometry Centre, Institute of Chemistry, University of Rostock, Rostock, Germany

Abstract Radiocarbon (^{14}C) analysis is a unique tool to distinguish fossil/nonfossil sources of carbonaceous aerosols. We present ^{14}C measurements of organic carbon (OC) and total carbon (TC) on highly time resolved filters (3–4 h, typically 12 h or longer have been reported) from 7 days collected during California Research at the Nexus of Air Quality and Climate Change (CalNex) 2010 in Pasadena. Average nonfossil contributions of 58% ± 15% and 51% ± 15% were found for OC and TC, respectively. Results indicate that nonfossil carbon is a major constituent of the background aerosol, evidenced by its nearly constant concentration (2–3 μgC m^{-3}). Cooking is estimated to contribute at least 25% to nonfossil OC, underlining the importance of urban nonfossil OC sources. In contrast, fossil OC concentrations have prominent and consistent diurnal profiles, with significant afternoon enhancements (~3 μgC m^{-3}), following the arrival of the western Los Angeles (LA) basin plume with the sea breeze. A corresponding increase in semivolatile oxygenated OC and organic vehicular emission markers and their photochemical reaction products occurs. This suggests that the increasing OC is mostly from fresh anthropogenic secondary OC (SOC) from mainly fossil precursors formed in the western LA basin plume. We note that in several European cities where the diesel passenger car fraction is higher, SOC is 20% less fossil, despite 2–3 times higher elemental carbon concentrations, suggesting that SOC formation from gasoline emissions most likely dominates over diesel in the LA basin. This would have significant implications for our understanding of the on-road vehicle contribution to ambient aerosols and merits further study.

1. Introduction

Particulate matter (PM) in ambient air has a negative impact on human health because it can cause respiratory and cardiopulmonary diseases that lead to increased mortality [*Pope and Dockery*, 2006; *World Health Organization*, 2006]. Aerosol particles also affect the climate by scattering and absorbing sunlight and modifying clouds [*Intergovernmental Panel on Climate Change*, 2007; *Jacobson et al.*, 2000]. Carbonaceous particles (total carbon, TC) are a major fraction of the fine aerosol (PM_1 or $PM_{2.5}$, PM < 1 or 2.5 μm) and contribute from 10% up to 90% of the PM mass depending on the location and season [*Gelencsér*, 2004; *Jimenez et al.*, 2009; *Putaud et al.*, 2004]. TC is further classified into the subfractions elemental carbon (EC) and organic carbon (OC) [*Jacobson et al.*, 2000]. EC is directly emitted from combustion processes of fossil and nonfossil fuels (e.g., coal, gasoline, diesel, oil, and biomass) [*Pöschl*, 2005]. OC, on the other hand, can be directly emitted as primary organic aerosol (POA) from biogenic sources (e.g., plant debris), biomass burning, cooking, and fossil fuel combustion or can be formed in the atmosphere as secondary organic aerosol (SOA) via gas-to-particle conversion of low-volatility reaction products of gas phase precursors [*Hallquist et al.*, 2009; *Jacobson et al.*, 2000]. As a result, organic aerosol (OA) is comprised of an immensely complex mixture of POA and SOA compounds from a myriad of sources [*Jimenez et al.*, 2009]. The characterization of these sources and the quantification of their

emission strengths is a key step in understanding the impact of OA on public health and climate and improving the implementation of effective mitigation strategies.

Several measurement techniques and methods exist for the characterization and quantification of POA and SOA. One among those is the Aerodyne aerosol mass spectrometer (AMS) which measures the nonrefractory organic and inorganic (sulfate, nitrate, chloride, and ammonium) composition of submicron particles [*Jimenez et al*., 2003; *Drewnick et al*., 2005; *DeCarlo et al*., 2006; *Canagaratna et al*., 2007]. Positive matrix factorization (PMF) of the AMS organic mass spectra [*Paatero and Tapper*, 1994; *Lanz et al*., 2007; *Ulbrich et al*., 2009] can then be used to retrieve different OA sources and formation processes. However, it is not possible to assign an anthropogenic versus biogenic or fossil versus nonfossil contribution for OA sources with PMF, especially for SOA.

Radiocarbon analysis (^{14}C) is a quantitative tool for unambiguously distinguishing fossil and nonfossil sources of EC and OC. ^{14}C is completely depleted in fossil fuel emissions (^{14}C half-life = 5730 years), which can therefore be separated from nonfossil carbon sources (e.g., biomass burning, cooking, or biogenic emissions) which have a similar amount of ^{14}C as atmospheric carbon dioxide (CO_2) [*Szidat*, 2009; *Currie*, 2000]. The ^{14}C measurement on the EC fraction is still challenging. Only a few groups worldwide perform such analyses, and there are still open questions concerning the best approach for the EC isolation for ^{14}C measurements [*Zhang et al*., 2012; *Bernardoni et al*., 2013; *Dusek et al*., 2014]. However, a laboratory intercomparison shows that ^{14}C results of the OC and TC fraction agree well and are not sensitive to different isolation methods [*Szidat et al*., 2013].

Since ^{14}C measurements require a sufficient carbon loading, filters with sampling durations well over 12 h are typically analyzed. *Szidat et al*. [2004a, 2007] reported ^{14}C results obtained from aerosol filters with a sampling time of 12 h and 8 h, respectively, but in order to collect enough carbon, each filter was used during the same period of day (morning or evening) on one to three consecutive days. *Lewis and Stiles* [2006], *Klinedinst and Currie* [1999], and *Fushimi et al*. [2011] also used aerosol filters with relatively short sampling times (6–11.5 h) for ^{14}C analysis. In general, carbonaceous aerosol emission sources, formation processes, and sinks are exceedingly variable and their characterization thus requires highly time resolved measurements, which are often impractical for filter sampling.

Combining ^{14}C data with AMS-PMF results can help constrain the possible POA and SOA sources and precursors. Only a few studies [*Lanz et al*., 2008; *Aiken et al*., 2010; *Minguillón et al*., 2011] applied a combined ^{14}C/AMS-PMF source apportionment where the ^{14}C measurements were used to assign a fossil and nonfossil fraction to total SOA. However, only *Hodzic et al*. [2010] and *El Haddad et al*. [2013] presented such an apportionment of different SOA fractions.

In this study we present, to the best of our knowledge, the first highly time resolved (3–4 h) ^{14}C measurements. Filter samples collected during the California Research at the Nexus of Air Quality and Climate Change (CalNex) 2010 field campaign are analyzed to obtain diurnal profiles of fossil and nonfossil carbonaceous aerosols. When combined with organic markers measured by gas chromatography interfaced to mass spectrometry (GC-MS) and PMF analysis of aerosol mass spectra, the ^{14}C measurements provide detailed source apportionment of OA, especially focusing on SOA, in the Los Angeles basin. Some summarizing results were already shown in *Bahreini et al*. [2012] (6 h average fossil and nonfossil TC concentrations for 2 days). Here the full highly time resolved data set as well as new results and analysis are presented.

2. Methods

2.1. Aerosol Sampling

Filter sampling was conducted during the CalNex 2010 field campaign from 15 May to 16 June 2010 in Pasadena, CA (34.1405°N, 118.1225°W). The measurement site is located on the campus of the California Institute of Technology (Caltech), about 17 km northeast of downtown Los Angeles (LA) and 7 km south of the San Gabriel Mountains. The site is located within the LA basin, which has a population of about 18 million inhabitants (United States Census Bureau: http://www.census.gov). The region is influenced by multiple emission sources from traffic, cooking, industries, agriculture, biomass burning, and shipping [*Schauer et al*., 1996; *Williams et al*., 2010; *Wonaschutz et al*., 2011; *Bahreini et al*., 2012; *Hayes et al*., 2013]. The general wind pattern in the LA basin during daytime is driven by a sea breeze blowing onshore nearly perpendicular

to the coastline, developing around 11:00 and reaching the maximum in the afternoon [*Lu and Turco*, 1995]. This sea breeze advects emissions from the southwest toward the north and northeast of the LA basin. At night a land breeze develops above 200 m and lasts 5–6 h transporting air masses from the LA basin over the Santa Monica Bay [*Wagner et al*., 2012]. At the surface, the wind directions during the night were mostly southeast and the wind speeds were weaker than during the day [*Thompson et al*., 2012; *Hayes et al*., 2013]. The sea breeze/land breeze circulation prevailed during the sampling period as thoroughly described elsewhere [*Duong et al*., 2011; *Washenfelder et al*., 2011; *Thompson et al*., 2012; *Wagner et al*., 2012; *Hayes et al*., 2013]. Furthermore, the examination of the back trajectories showed that during the measurement period, the Pasadena measurement site was sometimes impacted by air masses from the California coastal mountain ranges to the north and northwest [*Hayes et al*., 2013].

PM_1 particles were collected onto preheated (8 h in air at 800°C in a muffle furnace, model LE 14/11/B150, Nabatherm, Germany) quartz fiber filters (Pallflex 2500QAT-UP) using a high-volume sampler (Digitel DHA-80, Switzerland), at a flow rate of 30 m^3h^{-1}. The sampling time was varied between 3 h (15–26 May and 4–15 June) and 4 h (26 May to 4 June) resulting in 6 to 8 filters per day. Immediately after sampling, the filters were wrapped in aluminum foil, sealed in plastic bags, and stored at −20°C until analysis. Field blank filters ($n = 4$) were also collected, following 15 min exposures to ambient air and treated in the same way as the loaded samples. Filter sampling has well known but nonsystematic artifacts due to adsorption and volatilization of semivolatile compounds [*Viana et al*., 2006; *Jacobson et al*., 2000]. Since it was not possible to conduct a more complex sampling (e.g., using two sampling lines, one with and without a denuder system for volatile OC removal or using two filters in series), artifacts could not be quantified. It has to be noted that due to the low-filter loadings caused by the short sampling times, such artifacts could have a larger influence than for studies with longer filter collection times.

2.2. ^{14}C Measurement

2.2.1. Selection of Filters

Filter samples from 7 days from the second half of the CalNex campaign with high OA concentrations (afternoon peak 15–24 μgm^{-3}) [see *Hayes et al*., 2013] were selected for the measurement of ^{14}C in TC and the determination of the fraction of nonfossil carbon therein ($f_{NF,TC}$). The second half of the campaign was more consistently impacted by urban pollution, with higher OA concentrations and consistent diurnal cycles, which was the target of our study, while during the first half of the CalNex campaign there was a period with higher dispersion and reduced impact of the urban emissions. Therefore, the results shown below are representative of days with high concentrations from the second half of the CalNex campaign and absolute concentrations represent an upper limit. ^{14}C in OC was additionally analyzed for 4 out of the 7 days selected. Only days with high concentrations were chosen because the analysis methods used (^{14}C analysis and EC/OC measurement) require a certain filter loading which was generally low due to the short sampling times. The reason for analyzing ^{14}C in OC for only 4 days was that there is also the possibility to calculate the nonfossil fraction of OC with the ^{14}C results of TC and the EC/OC concentrations (see section 2.2.5). This is because a comparison for measured and calculated values for nonfossil OC for the first four analyzed days showed really good agreement (see Figure 1). Therefore, we rather analyzed more days for ^{14}C in TC and performed repeated analysis of some samples for quality assurance instead of having both results, ^{14}C in OC and TC, for a smaller number of days. Table 1 indicates the chosen days, the sampling details, and the different types of analyses performed.

2.2.2. Sample Preparation

The sample preparation for the ^{14}C measurement was carried out using three different techniques, as summarized in Table 1.

First, OC was separated before ^{14}C analysis using the THEODORE system [see *Szidat et al*., 2004b for more details]. In brief, OC is oxidized to CO_2 from filter punches with a diameter of 11 to 16 mm at 340°C for 10 min in an oxygen stream. At this low temperature no significant amount of EC is expected to be released from the samples [*Szidat et al*., 2004b]. The evolving CO_2 is separated from interfering reaction gases, cryotrapped, and sealed in glass ampoules for ^{14}C measurements. TC samples are also prepared using the same system, where filter punches are combusted at 650°C for 12 min and the resulting CO_2 is recovered as described above.

Second, OC and TC samples were also combusted with a thermo-optical OC/EC analyzer (model 4L, Sunset Laboratory Inc., USA), which is equipped with a nondispersive infrared detector. The instrument is

modified such that it can be operated with pure oxygen as a carrier gas in addition to the conventionally used He and He/O_2 mixture. The temperatures and combustion times were set to the same values as used in the THEODORE protocol. The Sunset analyzer is connected to the trapping part of the THEODORE system, and the resulting CO_2 is recovered again as described above. A detailed description of this setup is described by *Zhang et al.* [2012], where it was shown that the results obtained using THEODORE and Sunset are comparable.

Third, TC samples for ^{14}C measurement were prepared following the approach described in *Fahrni et al.* [2010], where filter punches sealed in quartz tubes together with ~0.25 g of copper oxide (small rods for elemental analysis, Fluka, Switzerland) are combusted for 4 h at 800°C in a muffle furnace (model LE 14/11/B150, Nabatherm, Germany). Good agreement (± 5% on average) for the ^{14}C results was found between the samples prepared following this approach and those measured using THEODORE (see Figure S1 in the supporting information).

2.2.3. MICADAS Measurements

Carbonaceous fractions separated as described above were analyzed for ^{14}C content by the MIni radioCArbon DAting System (MICADAS) [*Synal et al.*, 2007] at the Swiss Federal Institute of Technology (ETH) Zürich. The instrument is equipped with a gas ion source [*Ruff et al.*, 2007; *Wacker et al.*, 2013], which allows direct CO_2 injection after dilution with He [*Ruff et al.*, 2010]. The fraction of modern carbon (f_M) is derived as the ratio of $^{14}C/^{12}C$ measured in the samples to the $^{14}C/^{12}C$ ratio in 1950, which is defined as 0.95 times the value of the standard SRM4990B [*Levin et al.*, 2010];

$$f_M = \left(^{14}C/^{12}C\right)_{\text{sample}} / \left(^{14}C/^{12}C\right)_{\text{AD1950}} \quad (1)$$

Values of f_M are corrected for $\delta^{13}C$ fractionation [*Wacker et al.*, 2010] and for the ^{14}C decay between 1950 and the year of measurement.

2.2.4. Data Correction and Presentation

Before using the f_M values obtained for source apportionment of fossil and nonfossil contributions, several corrections are carried out. First, a mass dependent blank correction is applied to the measured f_M following an isotopic mass balance approach [*Zapf et al.*, 2013]:

$$f_{M,\text{corr}} = \left(mC_{\text{sample}} \times f_{M,\text{sample}} - mC_{\text{blk}} \times f_{M,\text{blk}}\right) / \left(mC_{\text{sample}} - mC_{\text{blk}}\right) \quad (2)$$

where $f_{M,\text{corr}}$ is the blank-corrected f_M, and $f_{M,\text{sample}}$ and $f_{M,\text{blk}}$ are the f_M measured for samples and blanks, respectively. The carbon mass in the samples and the blanks are denoted by mC_{sample} and mC_{blk}, respectively. The mean TC concentration in the blank samples ($n = 4$) is 0.51 ± 0.23 μgC cm^{-2} with an f_M value for TC ($f_{M,\text{TC}}$) of 0.72 ± 0.24 (in general, throughout the manuscript, we always report average values ± standard deviation of the mean, unless it is indicated otherwise). Since no EC was detected in blank samples, the mean blank $f_{M,\text{TC}}$ and TC concentration were also used for the blank correction of the f_M values of OC ($f_{M,\text{OC}}$). The mean blank concentration contributes on average 17% ± 5% and 15% ± 4% to the OC and TC filter loading of the samples, respectively. The mass-dependent blank correction (see equation (2)) changes the measured f_M values on average by ±3% and increases the uncertainty by ~3%.

Second, to account for the thermonuclear weapon tests of the late 1950s and early 1960s which increased the radiocarbon content of the atmosphere [*Levin et al.*, 2010], $f_{M,\text{corr}}$ values obtained from equation (2) are converted into nonfossil fractions (f_{NF}), following equation (3) [*Szidat et al.*, 2006; *Zhang et al.*, 2012]

$$f_{\text{NF}} = f_{M,\text{corr}} / f_{\text{NF,ref}} \quad (3)$$

where $f_{\text{NF,ref}}$ is a reference value representing the modern ^{14}C content during the sampling period compared to 1950 before the bomb testing. The calculation of this parameter takes into account the contribution of biogenic (bio) and biomass burning (bb) sources to modern carbon:

$$f_{\text{NF,ref}} = p_{\text{bio}} \times f_{\text{bio,ref}} + (1 - p_{\text{bio}}) \times f_{\text{bb,ref}} \quad (4)$$

where $f_{\text{bio,ref}}$, the f_M reference value for biogenic aerosols, equals 1.036 ± 0.015 for 2010. It is taken from long-term $^{14}CO_2$ measurements at the background station Schauinsland [*Levin et al.*, 2010]. The f_M reference value for biomass burning aerosols $f_{\text{bb,ref}}$ is estimated as 1.116 ± 0.050 for 2010 using a tree growth model as described in *Mohn et al.* [2008]. The fraction of biogenic sources to the total nonfossil sources p_{bio} is assumed to be 0.9 ± 0.1 since no large biomass burning events were recorded during the measurement

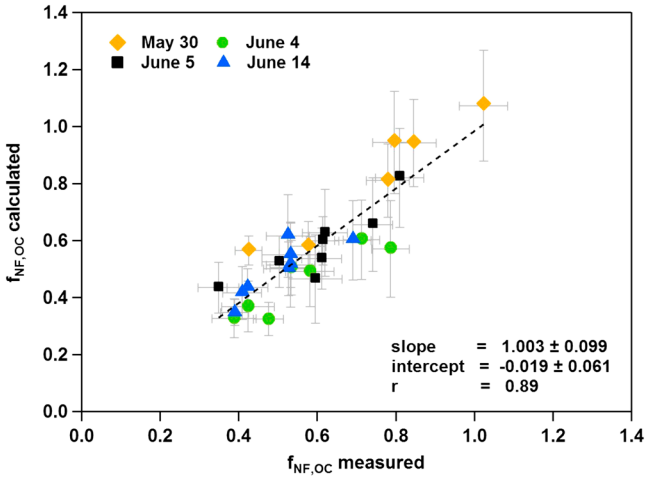

Figure 1. Linear least squares fit of the measured versus calculated $f_{NF,OC}$ values. The error bars for the measured $f_{NF,OC}$ represent the combined errors (1σ) of the ^{14}C measurement, the ^{14}C blank correction, and the ^{14}C bomb peak correction. In addition to these errors, the uncertainties of the OC and TC concentrations and the assumed $f_{NF,\ EC}$ are included in the error bars of the calculated $f_{NF,OC}$ (error propagation of equation (6)).

period. For $f_{bio,ref}$, $f_{bb,ref}$, and p_{bio} the uncertainties are reported which will be described in detail below (see section 2.2.6). *Hayes et al.* [2013] estimated the contribution of biomass burning OA to total OA to be at most 5% using AMS and Particle Analysis by Laser Mass Spectrometry (PALMS) as well as measurements of the biomass burning tracer acetonitrile. However, due to the uncertainties of these measurement techniques and the lack of tracers for identifying aged biomass burning particles, p_{bio} was set to 0.9 instead of 0.95. Note that p_{bio} has only a very little impact on $f_{NF,ref}$ compared to other measurement uncertainties (an increase of p_{bio} from 0.8 to 1 would change $f_{NF,ref}$ for this study only by 1.5%). Consequently, with a p_{bio} of 0.9 ± 0.1, an $f_{NF,ref}$ value of 1.044 with an uncertainty of ± 0.02 is calculated and ultimately used to determine the nonfossil fraction in OC and TC, $f_{NF,OC}$ and $f_{NF,TC}$, respectively.

2.2.5. Calculation of $f_{NF,OC}$

Radiocarbon in OC and thus $f_{NF,OC}$ was only measured for 4 days (see Table 1). However, for the days where these measurements were not available, $f_{NF,OC}$ was determined based on $f_{NF,TC}$ and EC/OC concentrations (see section 2.3), following equation (5) [*Szidat et al.*, 2004b]

$$TC \times f_{NF,TC} = OC \times f_{NF,OC} + EC \times f_{NF,EC} \quad (5)$$

Assuming a contribution of nonfossil carbon to EC, $f_{NF,EC}$, equation (5) can be expressed as

$$f_{NF,OC} = \left(f_{NF,TC} \times TC - EC \times f_{NF,EC}\right)/OC \quad (6)$$

A sensitivity analysis for the assumed $f_{NF,EC}$ covering a wide range of results (0–0.25; see Table S1 in the supporting information), including summer results from urban European cities, was carried out. Finally, a $f_{NF,EC}$ value of 0.1 ± 0.05, which is the average of several urban European cities in summer [*Szidat et al.*, 2006, 2009; *Minguillón et al.*, 2011], was chosen for the calculation of $f_{NF,OC}$. Good agreement was found between measured and calculated $f_{NF,OC}$ for the 4 days where both values are available (difference of $\pm 6.9\%$, slope ~1, and intercept ~0; see Figure 1). Therefore, the calculated $f_{NF,OC}$ will be presented in this study for the days where $f_{NF,OC}$ was not measured. Furthermore, the sensitivity analysis assuming different $f_{NF,EC}$ values shows that $f_{NF,OC}$ is only slightly affected by the assumed values and that the calculated $f_{NF,OC}$ values in this study are insensitive to a change in the biomass burning contributions to $f_{NF,EC}$.

Table 1. Sampling Details and Information on the Chosen Days and Different Offline Analysis Methods

	30 May	3 June	4 June	5 June	6 June	13 June	14 June
Day of the week	Sunday	Thursday	Friday	Saturday	Sunday	Sunday	Monday
Sampling time	4 h	4 h	3 h and 4 h	3 h	3 h	3 h	3 h
Analyses			*^{14}C in TC and EC/OC Concentrations*				
	^{14}C in OC	—	^{14}C in OC	^{14}C in OC	—	—	^{14}C in OC
	GC/MS	—	GC/MS	—	—	—	GC/MS
	AMS/PMF	AMS/PMF	AMS/PMF	AMS/PMF	AMS/PMF	AMS/PMF	AMS/PMF
^{14}C sample preparation technique	THEODORE/ Sunset	Sealed tube combustion	THEODORE	THEODORE/ Sunset	Sealed tube ombustion	THEODORE/ Sunset	THEODORE

It should be noted that there are differences in the car fleets between Europe (higher diesel car fraction) and the U.S. However, on the one hand, biomass burning influence during the CalNex campaign was negligible (see section 2.2.4 above) and on the other hand, $f_{NF,EC}$ was varied within a broad range in the sensitivity analysis which should account for possible differences (e.g., biodiesel fraction) between Europe and the U.S.

We also note that uncertainties associated with the calculation of $f_{NF,OC}$ are larger than for the days where it was measured which is mostly due to the large uncertainties of the EC/OC measurement caused by the low filter loadings (see section 2.2.6 and 2.3 below). This is also the reason why the calculation of $f_{NF,EC}$, for the days where $f_{NF,TC}$ and $f_{NF,OC}$ was measured, using equation (5), was not carried out since the uncertainties of the calculated $f_{NF,EC}$ would on average be 5 times higher than the value itself. The application of different thermal-optical protocols used for the EC/OC measurement on the calculation of $f_{NF,OC}$ is not expected to have a large impact due to the low EC/TC ratios during the campaign (on average ~12%). The assigned uncertainties used in the error propagation of equation (6) (see section 2.2.6 below) for the OC, EC, and TC concentrations are large and therefore should well represent possible differences due to different thermal-optical protocols (see section 2.3 below).

2.2.6. Uncertainty Assessment

The uncertainties (1 sigma) of $f_{NF,OC}$ and $f_{NF,TC}$ are the combined uncertainties from the ^{14}C measurement, the ^{14}C blank correction, and the ^{14}C bomb peak correction (see section 2.2.4). The uncertainty of the calculated $f_{NF,OC}$ (on average 14%; see section 2.2.5) was obtained by an error propagation of equation (6) and includes the uncertainties of the OC,EC, and TC mass concentration measurement (19%, 31%, and 19%, respectively; see section 2.3) as well as the uncertainty of $f_{NF,EC}$ (0.05; see section 2.2.5) and $f_{NF,TC}$ and is on average 9% higher than the average uncertainty of the measured $f_{NF,OC}$ values (5%). The average uncertainties of $f_{NF,OC}$ (measured and calculated values) and $f_{NF,TC}$ were calculated to be 9% and 5%, respectively. In the following, all individual uncertainties contributing to f_{NF} will be explained.

The average uncertainty of the measured f_M values of the samples presented in this study is 1.8% and is mainly driven by the counting statistics but also includes the variability of the standards and the background plus additional instrumental uncertainties [*Stuiver and Polach*, 1977; *Wacker et al*., 2010]. The uncertainty of $f_{M,corr}$ (the blank-corrected f_M) is on average 4.7%. It was derived from the error propagation of equation (2). This includes a conservative uncertainty of 30% for $f_{M,blk}$ to account for additional blank variability which was not covered by the blank filters [*Ceburnis et al*., 2011; *Dusek et al*., 2013]. The uncertainty of $f_{NF,ref}$ (0.02) is obtained by the error propagation of equation (4) and includes the uncertainties of $f_{bio,ref}$, $f_{bb,ref}$, and p_{bio}. The former was assumed to be 1.5% and includes a conservative estimation of the influence of primary biogenic OC, which could be older than the year of sampling and the natural variability of $^{14}CO_2$ [*Szidat et al*., 2006]. The uncertainty of $f_{bb,ref}$ was estimated by *Mohn et al*. [2008] to be 5% using a Monte Carlo simulation. The uncertainty of p_{bio} was set to 0.1 to account for uncertainties and single high events in the biomass burning contributions found by AMS and PALMS (see section 2.2.4).

2.3. EC/OC Measurements

All samples were measured for EC and OC content by a Sunset OC/EC analyzer, following the thermal-optical transmittance (TOT) protocol EUSAAR2 [*Cavalli et al*., 2010]. It has to be noted here that the OC/EC determination by TOT with thermal-optical instruments is not standardized yet and that different TOT protocols (e.g., NIOSH [*National Institute for Occupational Safety and Health*, 1999; *Peterson and Richards*, 2002], IMPROVE [*Chow et al*., 1993], and EUSAAR2 [*Cavalli et al*., 2010]) can lead to different results. TC measured with different protocols usually shows a good agreement (within 10%), whereas EC can differ significantly from method to method [*Chow et al*., 2001; *Schmid et al*., 2001; *Piazzalunga et al*., 2011]. However, since EC concentrations were really low (EC/TC ~12%), no large differences in OC due to different protocols are expected. The measurements were repeated 2 to 4 times depending on the variability caused by the relatively low filter loadings (maximum loading of 6.4 $\mu gC\ cm^{-2}$ and 1.6 $\mu gC\ cm^{-2}$ for OC and EC, respectively). In addition, a blank correction was carried out using the average of four blank filters ($TC = 0.51 \pm 0.23\ \mu gC\ cm^{-2}$). Since no EC was detected in blank samples, the mean TC concentration was also used for the blank correction of OC. The mean measurement uncertainty for OC, EC, and TC was estimated as 19%, 31%, and 19%, respectively, using the variability of all samples ($n = 18$) that were measured 4 times and the mean uncertainty of the blanks. This overall uncertainty is large and therefore should well represent possible differences due to different thermal-optical protocols.

2.4. AMS-PMF Data

A colocated Aerodyne high-resolution time-of-flight aerosol mass spectrometer (AMS) provided time-resolved measurements of nonrefractory organic and inorganic (sulfate, nitrate, chloride, and ammonium) submicron particles [*Jimenez et al*., 2003; *Drewnick et al*., 2005; *DeCarlo et al*., 2006; *Canagaratna et al*., 2007]. Positive matrix factorization (PMF) of the AMS organic mass spectra was used to retrieve OA sources and formation processes [*Paatero and Tapper*, 1994; *Lanz et al*., 2007; *Ulbrich et al*., 2009]. Details regarding the AMS operating conditions and PMF analysis can be found in *Hayes et al*. [2013]. Briefly, five components were identified by PMF. These include hydrocarbon-like organic aerosol (HOA), i.e., a surrogate for POA from fossil fuel combustion [*Lanz et al*., 2007; *Aiken et al*., 2008; *Jimenez et al*., 2009; *Ulbrich et al*., 2009], cooking-influenced organic aerosol (CIOA) [*Schauer et al*., 2002a; *Mohr et al*., 2012; *Crippa et al*., 2013a], local organic aerosol (LOA) [*Aiken et al*., 2009; *Docherty et al*., 2011; *Sun et al*., 2011] and semivolatile and low-volatility oxygenated organic aerosol (SV-OOA and LV-OOA), i.e., as surrogates for fresh and aged SOA, respectively [*Aiken et al*., 2008; *Jimenez et al*., 2009; *Ulbrich et al*., 2009].

2.5. Combined ^{14}C/AMS-PMF Source Apportionment

To gain more insight into the origin of SOA precursors, AMS-PMF results were combined with the ^{14}C measurements [*El Haddad et al*., 2013; *Minguillón et al*., 2011; *Aiken et al*., 2010; *Hodzic et al*., 2010; *Lanz et al*., 2008]. The approach is explained in the following.

The PMF factors are first converted from organic mass (OM) to OC using the OM:OC ratios determined from the elemental analysis of high-resolution AMS ($OM:OC_{HOA} = 1.3$, $OM:OC_{CIOA} = 1.4$, $OM:OC_{LOA} = 1.6$, $OM:OC_{SV\text{-}OOA} = 1.6$, and $OM:OC_{LV\text{-}OOA} = 2.2$) [*Hayes et al*., 2013]. For the OC mass concentration of the AMS factors, the following notations, hydrocarbon-like organic carbon (HOC), cooking-influenced organic carbon (CIOC), local organic carbon (LOC), semivolatile oxygenated organic carbon (SV-OOC), and low-volatility oxygenated organic carbon (LV-OOC), are adopted throughout the manuscript. OC measured offline by Sunset (OC_{Sunset}) and measured online by AMS (OC_{AMS}) are overall in good agreement, as shown in Figure S2 in the supporting information ($r = 0.86$). However, the slope between the two measurements indicates that the OC_{AMS} values exceed the ones of OC_{Sunset}. The average ratio OC_{AMS}/OC_{Sunset} is ~1.3. While the reason for this discrepancy remains uncertain at this stage, possible explanations include uncertainties in AMS and Sunset measurements (± 30% for AMS [*Hayes et al*., 2013; *Middlebrook et al*., 2012] and ± 19% for Sunset), evaporation losses of semivolatile compounds from filter samples and uncertainties related to the determination of AMS OM/OC ratios.

Second, the nonfossil fraction of the sum of OC_{AMS} and EC ($TC_{NF,AMS}$) is calculated by multiplying it with $f_{NF,TC}$ from the ^{14}C measurement.

$$TC_{NF,AMS} = (OC_{AMS} + EC) \times f_{NF,TC} \tag{7}$$

Third, a fossil/nonfossil fraction was assumed a priori for the primary PMF factors HOC, CIOC, and LOC as well as for EC. The sources of EC, HOC, and CIOC are relatively well constrained, whereas the origin of LOC is more uncertain (see section 3.3 below). The average nonfossil fraction of the PMF factors SV-OOC ($f_{NF,SV\text{-}OOC}$) and LV-OOC ($f_{NF,LV\text{-}OOC}$) is then derived by solving the following mass balance equation using a multiple linear regression analysis:

$$\begin{aligned} TC_{NF,AMS} - f_{NF,HOC} \times HOC - f_{NF,CIOC} \times CIOC - f_{NF,LOC} \times LOC - f_{NF,EC} \times EC = \\ f_{NF,LV\text{-}OOC} \times \text{LV-OOC} + f_{NF,SV\text{-}OOC} \times \text{SV-OOC} \end{aligned} \tag{8}$$

In this method, all the nonfossil fractions of the PMF factors and EC are assumed to be constant, even though these, especially $f_{NF,LV\text{-}OOC}$ and $f_{NF,SV\text{-}OOC}$, may vary over the course of the sampling period. However, in the absence of additional information, this approach provides the best estimate of contributions of fossil and nonfossil sources to the PMF factors averaged for the measurement period, without introducing additional degrees of freedom in the regression method that can result in additional uncertainties.

A sensitivity analysis for the calculated $f_{NF,LV\text{-}OOC}$ and $f_{NF,SV\text{-}OOC}$ was performed using a pseudo Monte Carlo simulation by varying all the a priori-assumed factors ($f_{NF,HOC}$, $f_{NF,CIOC}$, $f_{NF,LOC}$, and $f_{NF,EC}$) and also including the uncertainties of the ^{14}C and EC measurements. The detailed description about the defined range of the a priori-assumed factors and the uncertainties used in the pseudo Monte Carlo simulation as well as their influence on the result can be found in the supporting information.

2.6. Measurement of Organic Markers

The organic PM markers levoglucosan, polycyclic aromatic hydrocarbons (PAHs), oxygenated polycyclic aromatic hydrocarbons (o-PAHs), straight-chain alkanes (n-alkanes), and hopanes were measured for three complete days (see Table 1) using an in situ derivatization and thermal desorption method which is coupled to gas chromatography with mass selective detection (IDTD-GC-MS) (this method is described in detail in *Orasche et al.* [2011]). Briefly, the filter punches were placed into glass liners suitable for an automated thermal desorption unit [*Schnelle-Kreis et al.*, 2005]. Isotope-labeled standard compounds were spiked directly onto the filter surface to account for influences of the matrix for later quantification. Derivatization was performed on the filter by adding of liquid derivatization reagent N-methyl-N-trimethylsilyl-trifluoroacetamide (MSTFA, Macherey-Nagel, Germany). During 16 min of desorption time, in addition, an in situ derivatization with gaseous MSTFA was carried out to quantitatively silylate polar organic compounds and optimize the desorption process. The derivatization procedure has been automated as well. Derivatized and desorbed molecules were first trapped on a precolumn before separation by gas chromatography (BPX-5 capillary column, SGE, Australia). The detection and quantification of compounds was carried out on a Pegasus III time-of-flight mass spectrometer using the ChromaTOF software package (LECO, St. Joseph, MI).

3. Results and Discussion

3.1. Fossil and Nonfossil Fractions of TC and OC

Figure 2 presents the results for $f_{NF,OC}$ and $f_{NF,TC}$ for all days analyzed. The data for all the individual filter samples including the raw data from the ^{14}C measurement are listed in Table S2 in the supporting information. The total average of $f_{NF,TC}$ (0.51 ± 0.15; individual values range from 0.29 to 1.00) was found to be slightly lower than the average of $f_{NF,OC}$ (0.58 ± 0.15, 0.32–1.03), due to the contribution of fossil fuel emissions to EC. The average of $f_{NF,OC}$ including only the days where it was measured (see Table 1) is 0.60 ± 0.17 and is statistically not different (*t* test, 95% confidence interval) from the average overall values (measured and calculated). Given the low contribution of biomass burning during the measurement period (see section 2.2.4 above), this result reveals the significant contribution of nonfossil sources such as biogenic SOA and cooking to atmospheric OA, despite extensive fossil emissions in the region (i.e., more than 50% of OC is nonfossil). Very similar ^{14}C results ($f_{NF,TC}$ ~0.47) for the annual average of 2007 were reported for Wilmington, a district of LA adjacent to the ports of Los Angeles and Long Beach [*Buchholz et al.*, 2012]. Previous ^{14}C data reported from two stations for this region (in Long Beach and Azusa) in 1982 (four filters for each location with a sampling time of 3 months covering the whole year from January to December) suggest lower relative contributions from nonfossil sources (0.32–0.43 and 0.2–0.35) [*Hildemann et al.*, 1994]. It is noted that while the absolute concentration of nonfossil TC (TC_{NF}) remained relatively constant between 1982 and 2010 (~3 $\mu gC\ m^{-3}$), a noticeable decrease is observed in fossil TC (TC_F) during this time period (~7 $\mu gC\ m^{-3}$ in 1982 compared to ~3 $\mu gC\ m^{-3}$ in 2010). This decrease is expected considering the air quality mitigation strategies implemented since 1982.

The most prominent feature in Figure 2 is the f_{NF} diurnal pattern, with increasing values during the night and early morning (on average 0.71 ± 0.12 for $f_{NF,OC}$ and 0.60 ± 0.15 for $f_{NF,TC}$) and clear minima in the early afternoon (0.42 ± 0.08 and 0.38 ± 0.09 for $f_{NF,OC}$ and $f_{NF,TC}$, respectively), coinciding with the transport of the western LA basin plume to Pasadena by the sea breeze. The diurnal patterns for all the selected days are similar, and the variability of the average diurnal cycle (standard deviation of the mean) is 5–14% for $f_{NF,OC}$ and 3–12% for $f_{NF,TC}$ (see Figure 2, left). Nevertheless, it should be noted that two samples from 5 June and all samples from 30 May show exceptionally higher nonfossil fractions (24 h average of $f_{NF,OC}$ is 19% and $f_{NF,TC}$ is 30% higher on 30 May; the average for both $f_{NF,OC}$ and $f_{NF,TC}$ for the two samples on 5 June from 09:00 to 12:00 is 25% higher than for the other days). The measurements of those filters were performed several times, excluding possible contamination during sample preparation. The elevated f_{NF} appears consistent with an increase in the OC/EC and OM/HOA ratios (by a factor of ~2) during 30 May, suggesting an additional input from nonfossil sources to OC. Furthermore, levoglucosan concentrations on 30 May are a factor of ~2 higher than on 4 June and 14 June (see Figure S3). These findings suggest that enhanced charbroiling could be the reason for the higher f_{NF} values, since in 2010, 30 May was the Sunday before the Memorial Day (a public holiday). No elevated f_{NF} values were found on the other two Sundays, 6 June and 13 June. *Buchholz*

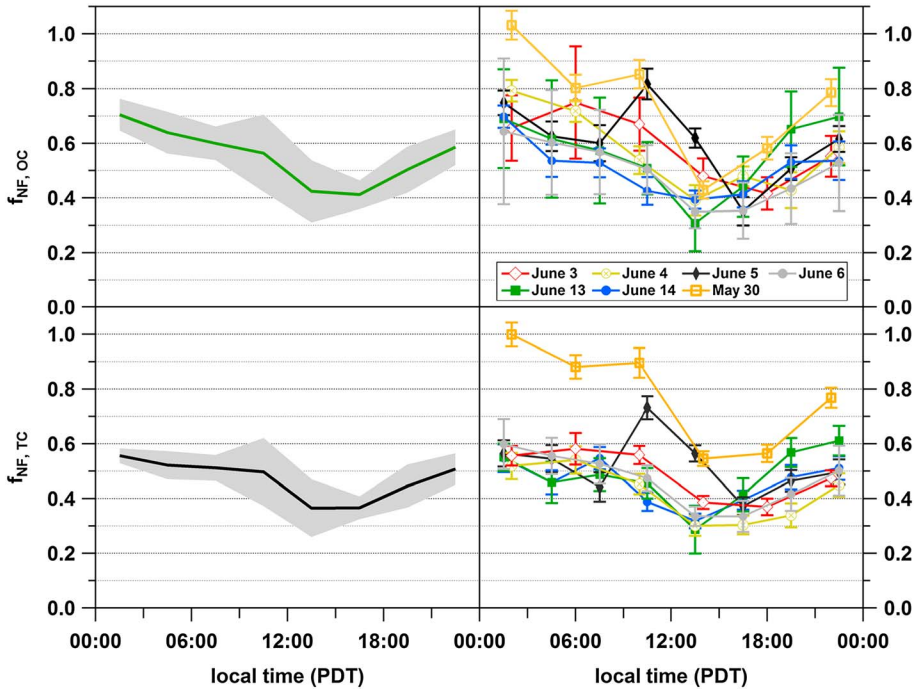

Figure 2. Diurnal cycle of nonfossil (top) OC and (bottom) TC. The time on the *x* axis represents the midpoint of the sampling interval. (left) The average diurnal cycle and (right) the results for the individual days. In the average diurnal cycle, 30 May is excluded (see section 3.1). The error bars are the combined errors (1σ) from the ^{14}C measurement, the ^{14}C blank correction, and the ^{14}C bomb peak correction. The grey-shaded area in Figure 2 (left) marks the day-to-day variation.

et al. [2012] identified anthropogenic inputs of TC in the LA basin close to the port of Long Beach with excessive ^{14}C content ($f_{NF,TC}$ values of up to 3.4). However, sources of anthropogenic ^{14}C are unlikely the reason for the elevated f_{NF} values on 30 May and 5 June due to the following reasons:

1. No f_{NF} values >1 were measured in Pasadena in this study, whereas almost all samples in *Buchholz et al*. [2012], which showed anthropogenic ^{14}C inputs (8 out of 34), exhibit f_{NF} values of >1.4.
2. A contamination during handling before and after the filter sampling before filters were frozen and shipped to Switzerland can be excluded since filters from no other day show elevated f_{NF} values, and it is very unlikely that an artificial ^{14}C source would contaminate only samples from 1 day during handling.
3. ^{14}C results from the measured blank filters ($n=4$) showed no elevated $f_{NF,TC}$ values (results range from 0.62 to 0.88) including one blank from 30 May ($f_{NF,TC}=0.75$).
4. Anthropogenic sources of ^{14}C (nuclear power plants, pharmaceutical industry, biochemical laboratories, …) are point sources and show a high temporal variability. Therefore, the high time resolution filter sampling conducted in this study together with the consistent daily change in wind direction (land/see breeze system) would be ideal to detect such inputs. However, f_{NF} values of all analyzed days show very consistent diurnal cycles without large increases in the data.
5. The distance between Pasadena and Long Beach is large (~40 km), and *Buchholz et al*. [2012] stated that sources of anthropogenic ^{14}C with distances of >50 km to the sampling site are unlikely to have a large influence on ^{14}C results of aerosol filter samples.

Nevertheless, since 30 May shows clearly different f_{NF} values than the other days and as we cannot completely rule out a low contribution from sources emitting anthropogenic ^{14}C during that day, this period was excluded from the analyses below. No anomalous OC/EC and OM/HOC ratios were found during 5 June compared to the other days to explain the unexpected nonfossil amplitude around noon, and therefore, the results from these two filter samples were included in the average diurnal cycle. As shown in Figure S4 (see supporting information), considering 30 May in the average has only a slight influence on the results ($f_{NF,OC}$ and $f_{NF,TC}$ are 5% and 6% more modern, and the variability increases from 8% to 12% and from 7% to 13% for $f_{NF,OC}$ and $f_{NF,TC}$, respectively). We note that anthropogenic sources of modern carbon such as

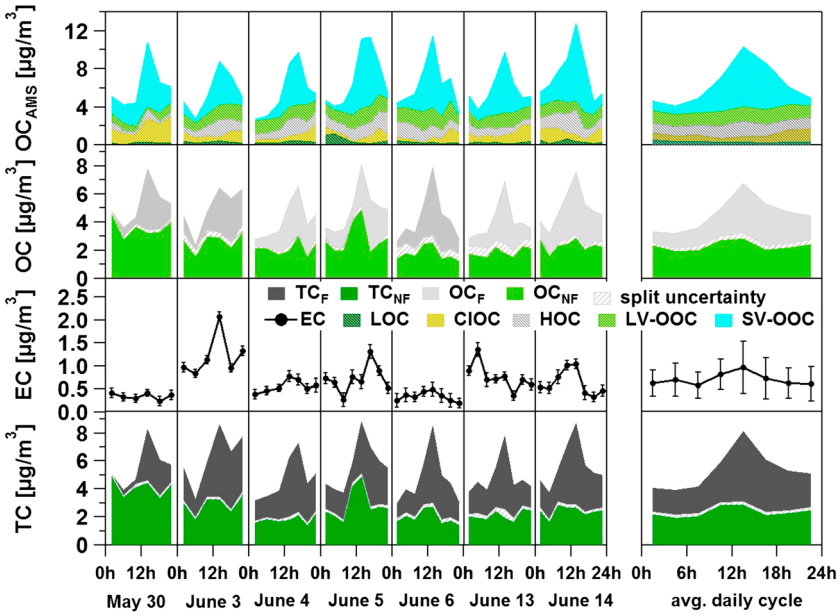

Figure 3. Fossil and nonfossil OC and TC as well as EC and PMF factor concentrations for (left) the individual days and (right) the average diurnal cycles. The time on the *x* axis represents the midpoint of the sampling interval. In the average diurnal cycle, 30 May is excluded (see section 3.1). The error bars for EC for the individual days represent the assigned uncertainty of the individual EC measurements (see section 2.3), and the error bars of average diurnal cycle for EC represent the variability. The split uncertainty of the individual days is calculated by multiplying the uncertainty of the f_{NF} values with the OC and TC concentrations and gives the error of the split into the fossil and nonfossil concentrations. The split uncertainty of the average diurnal cycle is the propagated error (1σ) of the individual days.

those identified by *Buchholz et al.* [2012] could potentially increase the background ^{14}C levels slightly. A 10% increase of the background ^{14}C (i.e., $f_{NF,ref}$ in equation (3) increases from 1.04 to 1.14), which is unlikely due to the highly variable emissions of only a few anthropogenic ^{14}C point sources, would decrease the f_{NF} values on average by only ~5%. In view of this result, the absence of emission inventories for anthropogenic ^{14}C sources enabling an accurate assessment of their influence, and as there is no evidence in our data that would point out to such contamination (see discussion above), we will not consider such correction in the following.

We also tested possible differences in the average diurnal cycle of $f_{NF,OC}$ using only the data from the measured days versus including all data (measured and calculated). As shown in Figure S5 (see supporting information) there are no significant differences between the two different average diurnal cycles. It should also be noted that only 7 days with high OA concentrations (on average 10.6 μgm^{-3}) were selected. However, the relative fossil and nonfossil OC and TC contributions from the seven selected days which exhibit high OA concentrations may be considered representative of the second half of the CalNex campaign since the average relative contribution of the different sources to OA (HOA ~14%, LOA ~5%, CIOA ~12%, LV-OOA ~28%, and SV-OOA ~40%) and EC/OA (6%) for the seven selected days are very similar to the campaign average from 15 May to 16 June 2010 (HOA/OA ~12%, LOA/OA ~5%, CIOA/OA ~17%, LV-OOA/OA ~32%, SV-OOA/OA ~34%, and EC/OA ~7%) [see *Hayes et al.*, 2013]. Furthermore, days from the second half of the CalNex campaign (also days with lower concentrations) show a very similar diurnal pattern (total OA and PMF factors), and also, the campaign average diurnal cycle of the PMF factors is very much consistent to the one obtained here [see *Hayes et al.*, 2013] (section 3.3.2 below), signifying that OA dynamics may be driven by the same sources/processes.

3.2. Levels and Variability of Fossil and Nonfossil Carbon

Combining the ^{14}C and OC/EC measurements gives access to the absolute concentrations of fossil and nonfossil OC and TC, whose time series and diurnal profiles are presented together with those of EC and PMF factors in Figure 3. OC and TC concentrations consistently rise during the day, with local maxima that extend from about 13:30 to 16:30 (6.5–8.1 $\mu gC\ m^{-3}$ and 7.1–8.8 $\mu gC\ m^{-3}$ for OC and TC, respectively),

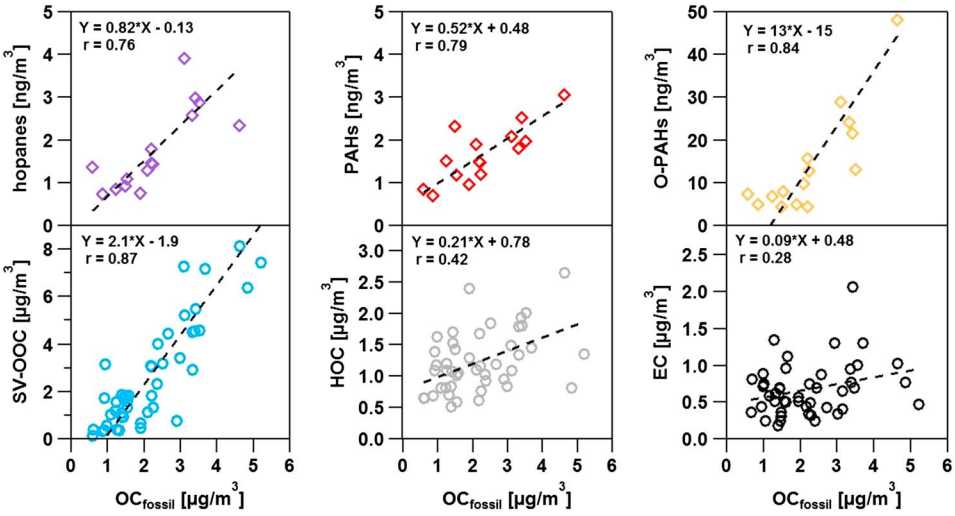

Figure 4. Scatterplots of the PMF factors SV-OOC, HOC, and EC (bottom) as well as the total mass concentration of the organic markers hopanes, PAHs, and o-PAHs versus OC_F (top). The organic marker data include only results from 2 days, whereas the AMS/PMF and ^{14}C data represent results from 6 days; 30 May is excluded (see section 3.1). An orthogonal distance regression was used to fit the data. The correlation between o-PAHs and OC_F is hardly influenced if the single high data point of the o-PAHs is excluded (correlation coefficient and slope decrease by only 10% to 0.76 and by 15% to 11, respectively).

and coincide with the arrival of the western LA basin plume. The lowest OC and TC concentrations are observed during the night and early morning (2.4–3.6 µgC m^{-3} and 3.0–3.9 µgC m^{-3} for OC and TC, respectively). The EC concentration is on average 0.6 ± 0.4 µgC m^{-3} (0.2–2.1 µgC m^{-3}) and accounts only for 12% ± 7% of TC. Examining the fossil and nonfossil origins of OC and TC clearly reveals that the nonfossil concentrations remain relatively constant throughout the day (see Figure 3). This indicates a nonfossil background of OC, ranging between 2 and 3 µgC m^{-3}, with a minor afternoon increase of ~1 µgC m^{-3} (~30%–50% compared to the nonfossil background). In contrast, the observed afternoon increase in OC and TC concentrations is found to mainly stem from fossil emissions, with an average increase in OC_F and TC_F concentrations of ~3 µgC m^{-3} (~230% and ~160% for OC_F and TC_F, respectively) compared to the average fossil concentrations from 0 h to 9 h. We recognize that the concentrations shown here represent most probably an upper limit for the CalNex campaign, since only days with high concentrations from the second half were selected for the analysis, where the measurement site was more consistently impacted by urban pollution.

Table 2. Pearson Correlation Coefficient for the Regression Analysis of the PMF Factors and EC as Well as the Total Mass Concentrations of PAHs, o-PAHs, and n-alkanes Versus OC_{NF} and OC_F[a]

	OC_{NF}	OC_F
EC	0.35	0.28
SV-OOC	0.33	**0.87**
HOC	0.29	0.42
CIOC	−0.08	−0.02
LV-OOC	0.19	0.36
LOC	0.09	−0.16
Hopanes	0.02	**0.76**
PAHs	0.34	**0.79**
o-PAHs	0.31	**0.84**
n-alkanes	0.09	0.48

[a]Data from 30 May are excluded (see section 3.1). Correlation coefficients larger than 0.5 are marked in bold.

OC_F shows moderate or low correlation with EC ($r = 0.28$) and HOC ($r = 0.42$), although the latter two are directly emitted species from fossil fuel combustion mainly present in diesel exhaust emissions (see Figure 4 and Table 2). Instead, OC_F correlates more strongly with PAHs ($r = 0.79$) and hopanes ($r = 0.76$) which are other primary fossil fuel combustion markers [*Robinson et al.*, 2006; *Subramanian et al.*, 2006]. These results suggest that OC_F may have a higher contribution from sources with elevated PAHs and hopanes, versus sources with significant concentrations of EC. This would be expected from sources such as gasoline vehicles [*Schauer et al.*, 2002b]. Furthermore, these high correlations between the PAHs and hopanes with OC_F demonstrate again the influence of the transport of the emissions of the western LA basin to Pasadena with the sea breeze. Additionally, OC_F correlates also really well with SV-OOC ($r = 0.87$) and o-PAHs ($r = 0.84$), which both show

increasing contributions in the early afternoon (see Figures 4 and S6). These significant correlations of OC_F with secondary species together with their much higher concentrations compared to primary species (e.g., o-PAHs/(PAHs + hopanes) ~3) indicate that the increase of the OC concentration for the selected days in the early afternoon is mainly due to fresh anthropogenic SOC transported to Pasadena and formed within the western LA plume from fossil precursors. Combined with the low correlation between OC_F and EC and the fact that we do not observe a weekend to weekday difference in the OC_F levels and fractions, which would be expected due to the well-known large decrease of on-road diesel vehicle activity in the LA basin and thus significantly reduced specific VOCs emissions [*Marr and Harley*, 2002; *Pollack et al*., 2012], this observation supports the suggestions of *Bahreini et al*. [2012] and *Hayes et al*. [2013] that gasoline emissions may play a larger role than diesel emissions in the production of anthropogenic SOA in the LA basin. However, it should be noted that the correlation between OC_F and the organic markers (PAHs, o-PAHs and hopanes; see Figure 4 (top)) includes less data than the correlation between OC_F and the AMS/PMF data. In the next section, we assess the relative contribution of fossil and nonfossil precursors in the production of fresh and aged SOA.

3.3. Combined ^{14}C/AMS-PMF Source Apportionment

3.3.1. Range and Sensitivity of Results

Additional insights into the sources of OC can be gained by combining ^{14}C measurements with AMS/PMF results. A major goal for the CalNex experiment is to improve the understanding of the formation and sources of SOA in California. The work presented in this section makes a contribution toward this goal by quantifying the fossil and nonfossil fractions of the secondary PMF factors, SV-OOC and LV-OOC. This apportionment was achieved using a multiple regression analysis (see equation (8)), as described in section 2.5. In the analysis, the fossil and nonfossil origins of the three primary PMF factors (CIOC, HOC, and LOC) and EC are assumed a priori, where $f_{NF,CIOC}$, $f_{NF,HOC}$, and $f_{NF,LOC}$ as well as $f_{NF,EC}$ denote the nonfossil fraction in CIOC, HOC, LOC and EC, respectively. The sensitivity of the analysis outputs to these assumptions is examined via a pseudo Monte Carlo simulation by varying $f_{NF,CIOC}$, $f_{NF,HOC}$, $f_{NF,LOC}$, and $f_{NF,EC}$ in equation (8) within a predetermined range. This yields a range of nonfossil LV-OOC and SV-OOC fractions ($f_{NF,LV\text{-}OOC}$ and $f_{NF,SV\text{-}OOC}$, respectively), which are plotted in Figure S7. A detailed description about the predetermined range of the a priori-assumed nonfossil fractions and uncertainties which were fed into the pseudo Monte Carlo simulation as well as their effects on the results can be found in the supporting information.

In brief, it appears that $f_{NF,SV\text{-}OOC}$ is insensitive while $f_{NF,LV\text{-}OOC}$ is quite sensitive to the a priori-assumed nonfossil fractions (see Figure S7). An increase/decrease of 0.1 of $f_{NF,CIOC}$, $f_{NF,HOC}$, $f_{NF,LOC}$, and $f_{NF,EC}$ changes $f_{NF,LV\text{-}OOC}$ by ± 6%, 3%, 7%, and 4%, respectively, whereas $f_{NF,SV\text{-}OOC}$ is modified by less than 1%. It should be noted though that a lot of combinations yield "unrealistic" values for $f_{NF,LV\text{-}OOC} > 1$, but for realistic combinations, the analysis shows that $f_{NF,LV\text{-}OOC}$ never decreases below 0.69, even for very high contributions of nonfossil carbon assumed for the primary fractions (e.g., $f_{NF,CIOC} = 1$ $f_{NF,HOC} = 0.1$, $f_{NF,LOC} = 1$, and $f_{NF,EC} = 0.2$). This illustrates that LV-OOC, a proxy for aged SOC, is dominated by nonfossil precursors. By contrast, the oxidation of fossil emissions seems to produce substantial amounts of fresh fossil SOC, significantly contributing to SV-OOC, on average by 71%. An advantage of the pseudo Monte Carlo simulation used here is that it clearly shows that this difference in the origin of SV-OOC and LV-OOC is observed independently of the assumptions and the uncertainties related to the calculation.

The uncertainties of $f_{NF,SV\text{-}OOC}$ and $f_{NF,LV\text{-}OOC}$ ($f_{NF,OOC}$) are defined as the maximum change in the corresponding $f_{NF,OOC}$ due to changes in the a priori assumptions and/or the consideration of the uncertainties of $f_{NF,TC}$ and/or $f_{NF,EC}$ as well as EC and are estimated by the simulation on average to be 18% for $f_{NF,LV\text{-}OOC}$ and 3% for $f_{NF,SV\text{-}OOC}$ (see Figure S7 in the supporting information).

3.3.2. Best Estimate

Figure 5 presents our best estimate of the fossil and nonfossil contributions to the PMF factors for the seven selected days, illustrated as an average diurnal cycle. In this solution $f_{NF,HOC}$ and $f_{NF,EC}$ were set to 0.05 and 0.1, respectively, to account for the utilization of biofuels (see supporting information). The value 0.1 for the latter also represents the average of ^{14}C measurements of EC from several urban European areas in summer. Fraction $f_{NF,LOC}$ was fixed at 0.5 since the origin of LOC is not known (see supporting information), and considering its small contribution (~5% of OC_{AMS} mass), different $f_{NF,LOC}$ values do not have a large effect on the calculation of $f_{NF,LV\text{-}OOC}$ and $f_{NF,SV\text{-}OOC}$ (a change of $f_{NF,LOC}$ by ± 0.3 would lead to an increase/decrease of

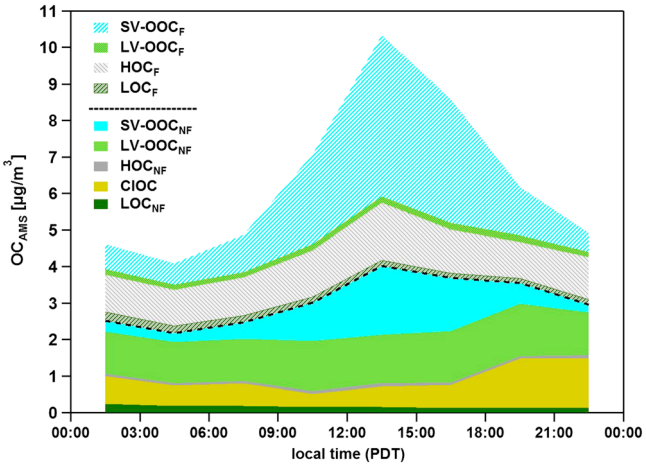

Figure 5. Average diurnal cycles of the fossil and nonfossil fractions of the PMF factors. The nonfossil fractions for HOC, CIOC, LOC, and EC were assumed to be 0.05, 1, 0.5, and 0.1, respectively. Fractions $f_{NF,LV\text{-}OOC}$ and $f_{NF,SV\text{-}OOC}$ were calculated (see equation (8)) to be 0.89 and 0.29, respectively. All nonfossil contributions are displayed below the black dashed line. In the average diurnal cycle, 30 May is excluded since the nonfossil values are significantly higher than for the other days.

$f_{NF,LV\text{-}OOC}$ and $f_{NF,LV\text{-}OOC}$ of 7.6% and <2%, respectively; see Figure S7). Considering these values, the only possible solution with $f_{NF,LV\text{-}OOC} < 1$ is obtained for $f_{NF,CIOC}$ equal 0.9 or 1. We consequently set $f_{NF,CIOC}$ to 1 which is expected if CIOC is completely due to nonfossil carbon in cooking emissions. Values of $f_{NF,LV\text{-}OOC}$ and $f_{NF,SV\text{-}OOC}$ were found to be 0.89 and 0.29, respectively. Note that this is the most likely solution, and that while $f_{NF,SV\text{-}OOC}$ is insensitive to assumption, $f_{NF,LV\text{-}OOC}$ can vary with the a priori assumptions, albeit with values strictly above 0.69.

From Figure 5, it appears that nonfossil OC is mainly composed of LV-OOC$_{NF}$, SV-OOC$_{NF}$, and CIOC$_{NF}$. CIOC$_{NF}$ contributes on average 13.9% ± 8.2% to total OC (0.77 ± 0.37 µgC m^{-3}) and increases in the evening due to enhanced cooking emissions into a shallower boundary layer. The model attributes the slight but regular increase (~1 µgC m^{-3}) observed in the nonfossil carbon (Figure 3) in the early afternoons to SV-OOC$_{NF}$. Such an increase could be due to SOC formed from local biogenic emissions, as has been previously reported at several locations and attributed to the daytime increase of biogenic emissions (mainly terpenes) and photochemical activities [*Slowik et al.*, 2010; *El Haddad et al.*, 2013] and/or due to SOC formation from cooking emissions, which can be substantial. This regular increase in nonfossil SV-OOA in the early afternoon may partially be induced by the anthropogenic emissions of NO_x, OH, and additional particle mass, which enhance SOA formation [*Donahue et al.*, 2006; *Hoyle et al.*, 2007, 2009]. The SV-OOC$_{NF}$ levels range from 0.22 µgC m^{-3} during the night to 1.89 µgC m^{-3} in the early afternoon and account on average for 10.8% ± 5.3% of OC$_{AMS}$ (0.77 ± 0.63 µgC m^{-3}).

LV-OOC$_{NF}$ concentrations show no or only a weak diurnal variation, indicative of an aged background aerosol, as opposed to a fresh SOA locally formed during midday peaks of photochemistry (see Figure 5). This is consistent with the findings by *Hayes et al.* [2013], showing the omnipresence of LV-OOC even in nonprocessed air masses and the association of OOA with aged OA in previous studies [*Jimenez et al.*, 2009]. Marine emissions might be suspected as a potential source of the background nonfossil OC, considering the proximity of our site to the Pacific and the observation of contributions from these emissions to biogenic OC in urban and marine environments [*Crippa et al.*, 2013b; *Ceburnis et al.*, 2011]. However, no important contribution of marine sources to PM_1 OC was found during the CalNex 2010 campaign [*Hayes et al.*, 2013]. Meanwhile, the examination of the back trajectories brings evidence that during the measurement period, the sampling site was sometimes impacted by air masses from the California coastal mountain ranges to the north and northwest where biogenic emissions are expected to be strong [*Hayes et al.*, 2013]. This suggests that most of the LV-OOC may be dominated by continental biogenic SOC which accounts to a large extent for the nonfossil background in the LA basin on the seven selected days presented here. LV-OOC$_{NF}$ contributes on average 1.28 ± 0.13 µgC m^{-3} (22.1% ± 5.2%) constituting the largest fraction (~30%) of OC$_{AMS}$ during nighttime and in the early morning.

Fossil OC is mainly composed of SV-OOC$_F$ and HOC$_F$. While HOC$_F$ (0.99–1.58 µgC m^{-3}) levels show a relatively small increase around midday (following the EC concentrations as they are both advected from the morning emissions in the downtown LA area), the large increase in fossil carbon contribution in the early afternoon is almost entirely attributed to SV-OOC$_F$ (0.51 µgC m^{-3} in the night and 4.42 µgC m^{-3} in the afternoon), which accounts for ~40% of the total OC at that time. This corroborates the above hypothesis that the increase in the PM concentrations after the arrival of the western LA basin plume to Pasadena is mainly caused by fresh anthropogenic SOC formed from fossil precursor gases.

While it is generally thought that much LV-OOC arises from additional aging of SV-OOC species [*Jimenez et al.*, 2009], the above discussion clearly shows that in the LA basin, for the seven selected days presented here, the two oxygenated factors derive from mostly distinct precursors. LV-OOC is overwhelmingly composed of nonfossil biogenic carbon (>69%), whereas a large fraction of SV-OOC is comprised of anthropogenic fossil secondary OC (SOC_F) (~71%), produced from fossil precursors within the western LA basin plume during advection to Pasadena. At least a fraction of the SV-OOC_{NF} is likely due to SOA formation from cooking emissions and thus is also anthropogenic. It is likely that the further oxidation of SV-OOC_F, which would produce LV-OOC_F can only be observed downwind of Pasadena. Overall, we conclude that in our conditions, 2.0 ± 1.5 μgC m^{-3} and 2.1 ± 0.7 μgC m^{-3} of SOC originate from fossil and nonfossil precursors, respectively. This implies that on a 24 h average basis, $56\% \pm 10\%$ of SOC ($33\% \pm 2\%$ of total OC_{AMS}) are related to local and regional biogenic and other nonfossil (e.g., cooking) SOA, despite extensive fossil fuel usage (traffic, industry, refineries, …) in the area.

3.3.3. Comparison With Results From Other Studies

The fossil contributions of SOC found in the LA basin on the seven selected days contrast significantly to the moderate levels reported for urban background stations in several European cities ($SOC_F = 0.5 \pm 0.4$ μg C m^{-3} and $SOC_{NF} = 1.2 \pm 0.2$ μgC m^{-3}, Barcelona [*Minguillón et al.*, 2011], Paris [*Freutel et al.*, 2013; *Crippa et al.*, 2013b], Marseille [*El Haddad et al.*, 2013], and Zürich [*Lanz et al.*, 2007, 2008; *Sandradewi et al.*, 2008]). At these European cities, the fraction of SOC_F to total SOC ($25\% \pm 13\%$ in Europe) is on average ~20% lower than in Pasadena, despite the higher EC concentrations ($EC_{Europe} = 1.9 \pm 0.8$ μgC m^{-3} versus $EC_{LA} = 0.6 \pm 0.4$ μgC m^{-3}). This, together with the higher fraction of gasoline cars in the U.S. compared to Europe, support the hypothesis proposed by *Bahreini et al.* [2012] and *Hayes et al.* [2013] and the findings in section 3.2 that gasoline emissions are likely to dominate over diesel in the formation of fossil SOA in the LA basin during the 7 days selected for this study. It has to be noted that possible different photochemical ages at the different locations were not taken into account for this comparison. However, *Platt et al.* [2013] found no significant changes in the SOA yields for gasoline cars after photochemical aging in chamber experiments after 4 h. Therefore, the different photochemical ages at the different stations may have a limited effect on the comparison of the fossil SOA levels.

4. Conclusions

In this study we provide time-resolved measurements of radiocarbon for OC and TC in PM_1 for seven selected days from the second half of the CalNex 2010 study at the Pasadena ground site located in the Los Angeles (LA) basin. To the best of our knowledge, this is for the first time that ^{14}C measurements were carried out on such highly time resolved ambient aerosol filter samples. As a consequence, a diurnal cycle for the fossil and nonfossil fractions of OC and TC could be demonstrated.

The results show a distinct and consistent diurnal pattern for all selected days. The nonfossil fractions are highest during nighttime and early mornings ($f_{NF,OC} = 0.71 \pm 0.12$ and $f_{NF,TC} = 0.60 \pm 0.15$ for TC from 24:00 to 06:00). In contrast, the carbonaceous aerosol is clearly influenced by fossil sources in the early afternoon (0.42 ± 0.08 and 0.38 ± 0.09 for $f_{NF,OC}$ and $f_{NF,TC}$, respectively), coinciding with the transport of the western LA basin plume to Pasadena by the sea breeze. The campaign average of 0.51 ± 0.15 for $f_{NF,TC}$ was found to be slightly lower than for $f_{NF,OC}$ (0.58 ± 0.15), due to the contribution of fossil fuel emissions to EC. OC and TC concentrations also show a clear diurnal cycle with a maximum after the arrival of the western LA plume. The nonfossil OC and TC concentrations stay nearly constant throughout the day (2–3 μgC m^{-3}), indicating a nonfossil background in the LA basin on the seven selected days. Furthermore, EC concentrations are low (0.6 ± 0.4 μgC m^{-3} on average) and show only a weak diurnal cycle. The afternoon increase of the concentrations primarily stems from fossil fuel combustion emissions since fossil OC and TC exhibit a strong increase (~3 μgC m^{-3}).

We combined the ^{14}C results with measurements of organic markers by gas chromatography mass spectrometry (GC-MS) and the source apportionment of OA by positive matrix factorization (PMF) analysis of aerosol mass spectrometry (AMS) data. The high correlation of fossil OC with semivolatile oxygenated organic carbon (SV-OOC) ($r = 0.84$), a surrogate for fresh secondary organic carbon (SOC), and the organic marker oxygenated polycyclic aromatic hydrocarbons (o-PAHs) ($r = 0.87$) indicate that the increase of the concentrations when the plume of the western LA basin arrives to Pasadena is mainly caused by fresh fossil

SOC. Furthermore, we were able to assign a nonfossil fraction to the secondary PMF factors semivolatile oxygenated organic carbon SV-OOC and low-volatility oxygenated organic carbon LV-OOC. The latter primarily (by >69%) stems from nonfossil sources, whereas SV-OOC is mainly (68%–74%) formed from fossil precursors. Cooking is estimated to contribute at least 25% of OC_{NF} (not accounting for possible SOA formation from this source), underlining the importance of urban nonfossil OC sources that are often ignored in such analyses.

Finally, the correlation between OC_F and the primary species EC ($r = 0.28$) and HOC ($r = 0.42$) is much weaker than for the secondary species. Furthermore, no weekend to weekday difference in the OC_F levels and fractions, which would be expected due to the well-known large decrease of on-road diesel vehicle activity on weekends in the LA basin and thus significantly reduced specific VOCs emissions, was observed. In addition, SOC_F levels and SOC_F to total SOC ratios for several European cities (Barcelona, Paris, Marseille, and Zürich), where the fraction of diesel passenger cars is higher than in the U.S., are on average lower by a factor of ~4 and 20%, respectively, despite the higher EC levels (2–3 times higher than in Pasadena). These findings corroborate the results of *Bahreini et al*. [2012] and *Hayes et al*. [2013] that gasoline emissions are likely to dominate over diesel in the formation of fossil SOA in the LA basin. This would have significant implications for our understanding of the contribution of on-road vehicles to ambient aerosols and merits further study.

Acknowledgments

Organization of the Pasadena ground site was led by the Jochen Stutz (University of California, Los Angeles) and John Seinfeld (California Institute of Technology, Caltech) as well as Joost de Gouw (National Oceanic and Atmospheric Administration, NOAA). Furthermore, we would like to thank CARB and NOAA for support of the site setup and the U.S. National Science Foundation (NSF) for the funding of the travel and shipping costs. José L. Jimenez and Patrick L. Hayes acknowledge support from CARB 08–319 and CARB 11–305 as well as DOE (BER, ASR Program) DE-SC0006035, DE-SC0006711, and DE-FG02-11ER65293. Patrick L. Hayes acknowledges a fellowship from the CIRES Visiting Fellows Program.

References

Aiken, A. C., et al. (2008), O/C and OM/OC ratios of primary, secondary, and ambient organic aerosols with high-resolution time-of-flight aerosol mass spectrometry, *Environ. Sci. Technol.*, *42*(12), 4478–4485, doi:10.1021/es703009q.

Aiken, A. C., et al. (2009), Mexico City aerosol analysis during MILAGRO using high resolution aerosol mass spectrometry at the urban supersite (T0)—Part 1: Fine particle composition and organic source apportionment, *Atmos. Chem. Phys.*, *9*(17), 6633–6653, doi:10.5194/acp-9-6633-2009.

Aiken, A. C., et al. (2010), Mexico City aerosol analysis during MILAGRO using high resolution aerosol mass spectrometry at the urban supersite (T0)—Part 2: Analysis of the biomass burning contribution and the non-fossil carbon fraction, *Atmos. Chem. Phys.*, *10*(12), 5315–5341, doi:10.5194/acp-10-5315-2010.

Bahreini, R., et al. (2012), Gasoline emissions dominate over diesel in formation of secondary organic aerosol mass, *Geophys. Res. Lett.*, *39*, L06805, doi:10.1029/2011GL050718.

Bernardoni, V., et al. (2013), Radiocarbon analysis on organic and elemental carbon in aerosol samples and source apportionment at an urban site in Northern Italy, *J. Aerosol Sci.*, *56*, 88–99, doi:10.1016/j.jaerosci.2012.06.001.

Buchholz, B. A., S. J. Fallon, P. Zermeño, G. Bench, and B. A. Schichtel (2012), Anomalous elevated radiocarbon measurements of PM2.5, *Nucl. Instrum. Methods Phys. Res., Sect. B*, *294*, 631–635, doi:10.1016/j.nimb.2012.05.021.

Canagaratna, M. R., et al. (2007), Chemical and microphysical characterization of ambient aerosols with the Aerodyne aerosol mass spectrometer, *Mass Spectrom. Rev.*, *26*(2), 185–222, doi:10.1002/mas.20115.

Cavalli, F., M. Viana, K. E. Yttri, J. Genberg, and J. P. Putaud (2010), Toward a standardised thermal-optical protocol for measuring atmospheric organic and elemental carbon: The EUSAAR protocol, *Atmos. Meas. Tech.*, *3*(1), 79–89, doi:10.5194/amt-3-79-2010.

Ceburnis, D., et al. (2011), Quantification of the carbonaceous matter origin in submicron marine aerosol by ^{13}C and ^{14}C isotope analysis, *Atmos. Chem. Phys.*, *11*(16), 8593–8606, doi:10.5194/acp-11-8593-2011.

Chow, J. C., J. G. Watson, L. C. Pritchett, W. R. Pierson, C. A. Frazier, and R. G. Purcell (1993), The DRI thermal optical reflectance carbon analysis system—Description, evaluation and application in United-States air-quality studies, *Atmos. Environ. Part A-Gen. Top.*, *27*(8), 1185–1201, doi:10.1016/0960-1686(93)90245-t.

Chow, J. C., J. G. Watson, D. Crow, D. H. Lowenthal, and T. Merrifield (2001), Comparison of IMPROVE and NIOSH carbon measurements, *Aerosol Sci. Technol.*, *34*(1), 23–34, doi:10.1080/02786201300081923.

Crippa, M., et al. (2013a), Wintertime aerosol chemical composition and source apportionment of the organic fraction in the metropolitan area of Paris, *Atmos. Chem. Phys.*, *13*(2), 961–981, doi:10.5194/acp-13-961-2013.

Crippa, M., et al. (2013b), Identification of marine and continental aerosol sources in Paris using high resolution aerosol mass spectrometry, *J. Geophys. Res. Atmos.*, *118*, 1950–1963, doi:10.1002/jgrd.50151.

Currie, L. A. (2000), Evolution and multidisciplinary frontiers of ^{14}C aerosol science, *Radiocarbon*, *42*, 115–126.

DeCarlo, P. F., et al. (2006), Field-deployable, high-resolution, time-of-flight aerosol mass spectrometer, *Anal. Chem.*, *78*(24), 8281–8289, doi:10.1021/ac061249n.

Docherty, K. S., et al. (2011), The 2005 study of organic aerosols at Riverside (SOAR-1): Instrumental intercomparisons and fine particle composition, *Atmos. Chem. Phys.*, *11*(23), 12,387–12,420, doi:10.5194/acp-11-12387-2011.

Donahue, N. M., A. L. Robinson, C. O. Stanier, and S. N. Pandis (2006), Coupled partitioning, dilution, and chemical aging of semivolatile organics, *Environ. Sci. Technol.*, *40*(8), 2635–2643, doi:10.1021/es052297c.

Drewnick, F., et al. (2005), A new time-of-flight aerosol mass spectrometer (TOF-AMS)—Instrument description and first field deployment, *Aerosol Sci. Technol.*, *39*(7), 637–658, doi:10.1080/02786820500182040.

Duong, H. T., A. Sorooshian, J. S. Craven, S. P. Hersey, A. R. Metcalf, X. Zhang, R. J. Weber, H. Jonsson, R. C. Flagan, and J. H. Seinfeld (2011), Water-soluble organic aerosol in the Los Angeles basin and outflow regions: Airborne and ground measurements during the 2010 CalNex field campaign, *J. Geophys. Res.*, *116*, D00V04, doi:10.1029/2011JD016674.

Dusek, U., H. M. ten Brink, H. A. J. Meijer, G. Kos, D. Mrozek, T. Röckmann, R. Holzinger, and E. P. Weijers (2013), The contribution of fossil sources to the organic aerosol in the Netherlands, *Atmos. Environ.*, *74*, 169–176, doi:10.1016/j.atmosenv.2013.03.015.

Dusek, U., M. Monaco, M. Prokopiou, F. Gongriep, R. Hitzenberger, H. A. J. Meijer, and T. Röckmann (2014), Evaluation of a 2-step thermal method for separating organic and elemental carbon for radiocarbon analysis, *Atmos. Meas. Tech. Discuss.*, *7*(1), 131–169, doi:10.5194/amtd-7-131-2014.

El Haddad, I., et al. (2013), Towards a better understanding of the origins, chemical composition and aging of oxygenated organic aerosols: Case study of a Mediterranean industrialized environment, Marseille, *Atmos. Chem. Phys.*, *13*(15), 7875–7894, doi:10.5194/acp-13-7875-2013.

Fahrni, S. M., H. W. Gäggeler, I. Hajdas, M. Ruff, S. Szidat, and L. Wacker (2010), Direct measurements of small 14C samples after oxidation in quartz tubes, *Nucl. Instrum. Methods Phys. Res., Sect. B*, *268*(7–8), 787–789, doi:10.1016/j.nimb.2009.10.031.

Freutel, F., et al. (2013), Aerosol particle measurements at three stationary sites in the megacity of Paris during summer 2009: Meteorology and air mass origin dominate aerosol particle composition and size distribution, *Atmos. Chem. Phys.*, *13*(2), 933–959, doi:10.5194/acp-13-933-2013.

Fushimi, A., et al. (2011), Radiocarbon (^{14}C) diurnal variations in fine particles at sites downwind from Tokyo, Japan in summer, *Environ. Sci. Technol.*, *45*(16), 6784–6792, doi:10.1021/es201400p.

Gelencsér, A. (2004), *Carbonaceous Aerosols*, Springer, Dordrecht.

Hallquist, M., et al. (2009), The formation, properties and impact of secondary organic aerosol: Current and emerging issues, *Atmos. Chem. Phys.*, *9*(14), 5155–5236, doi:10.5194/acp-9-5155-2009.

Hayes, P. L., et al. (2013), Organic aerosol composition and sources in Pasadena, California during the 2010 CalNex campaign, *J. Geophys. Res. Atmos.*, *118*, 9233–9257, doi:10.1002/jgrd.50530.

Hildemann, L. M., D. B. Klinedinst, G. A. Klouda, L. A. Currie, and G. R. Cass (1994), Sources of urban contemporary carbon aerosol, *Environ. Sci. Technol.*, *28*(9), 1565–1576, doi:10.1021/es00058a006.

Hodzic, A., J. L. Jimenez, A. S. H. Prévôt, S. Szidat, J. D. Fast, and S. Madronich (2010), Can 3-D models explain the observed fractions of fossil and non-fossil carbon in and near Mexico City?, *Atmos. Chem. Phys.*, *10*(22), 10,997–11,016, doi:10.5194/acp-10-10997-2010.

Hoyle, C. R., T. Berntsen, G. Myhre, and I. S. A. Isaksen (2007), Secondary organic aerosol in the global aerosol – chemical transport model Oslo CTM2, *Atmos. Chem. Phys.*, *7*(21), 5675–5694, doi:10.5194/acp-7-5675-2007.

Hoyle, C. R., G. Myhre, T. K. Berntsen, and I. S. A. Isaksen (2009), Anthropogenic influence on SOA and the resulting radiative forcing, *Atmos. Chem. Phys.*, *9*(8), 2715–2728, doi:10.5194/acp-9-2715-2009.

Intergovernmental Panel on Climate Change (2007), Fourth assessment report: The physical science basis, Working Group I, *Final Report*, Geneva, Switzerland. [Available at http://www.ipcc.ch/ipccreports/ar4-wg1.htm.]

Jacobson, M. C., H. C. Hansson, K. J. Noone, and R. J. Charlson (2000), Organic atmospheric aerosols: Review and state of the science, *Rev. Geophys.*, *38*(2), 267–294, doi:10.1029/1998RG000045.

Jimenez, J. L., et al. (2003), Ambient aerosol sampling using the Aerodyne aerosol mass spectrometer, *J. Geophys. Res.*, *108*(D7), 8425, doi:10.1029/2001JD001213.

Jimenez, J. L., et al. (2009), Evolution of organic aerosols in the atmosphere, *Science*, *326*(5959), 1525–1529, doi:10.1126/science.1180353.

Klinedinst, D. B., and L. A. Currie (1999), Direct quantification of $PM_{2.5}$ fossil and biomass carbon within the northern front range air quality study's domain, *Environ. Sci. Technol.*, *33*(23), 4146–4154, doi:10.1021/es990355m.

Lanz, V. A., M. R. Alfarra, U. Baltensperger, B. Buchmann, C. Hueglin, and A. S. H. Prévôt (2007), Source apportionment of submicron organic aerosols at an urban site by factor analytical modelling of aerosol mass spectra, *Atmos. Chem. Phys.*, *7*(6), 1503–1522, doi:10.5194/acp-7-1503-2007.

Lanz, V. A., et al. (2008), Source attribution of submicron organic aerosols during wintertime inversions by advanced factor analysis of aerosol mass spectra, *Environ. Sci. Technol.*, *42*(1), 214–220, doi:10.1021/es0707207.

Levin, I., T. Naegler, B. Kromer, M. Diehl, R. J. Francey, A. J. Gomez-Pelaez, L. P. Steele, D. Wagenbach, R. Weller, and D. E. Worthy (2010), Observations and modelling of the global distribution and long-term trend of atmospheric $^{14}CO_2$, *Tellus, Ser. B*, *62*(1), 26–46, doi:10.1111/j.1600-0889.2009.00446.x.

Lewis, C. W., and D. C. Stiles (2006), Radiocarbon content of $PM_{2.5}$ ambient aerosol in Tampa, FL, *Aerosol Sci. Technol.*, *40*(3), 189–196, doi:10.1080/02786820500521007.

Lu, R., and R. P. Turco (1995), Air pollutant transport in a coastal environment—II. Three-dimensional simulations over Los Angeles basin, *Atmos. Environ.*, *29*(13), 1499–1518, doi:10.1016/1352-2310(95)00015-q.

Marr, L. C., and R. A. Harley (2002), Spectral analysis of weekday-weekend differences in ambient ozone, nitrogen oxide, and non-methane hydrocarbon time series in California, *Atmos. Environ.*, *36*(14), 2327–2335, doi:10.1016/s1352-2310(02)00188-7.

Middlebrook, A. M., R. Bahreini, J. L. Jimenez, and M. R. Canagaratna (2012), Evaluation of composition-dependent collection efficiencies for the Aerodyne aerosol mass spectrometer using field data, *Aerosol Sci. Technol.*, *46*(3), 258–271, doi:10.1080/02786826.2011.620041.

Minguillón, M. C., et al. (2011), Fossil versus contemporary sources of fine elemental and organic carbonaceous particulate matter during the DAURE campaign in Northeast Spain, *Atmos. Chem. Phys.*, *11*(23), 12,067–12,084, doi:10.5194/acp-11-12067-2011.

Mohn, J., S. Szidat, J. Fellner, H. Rechberger, R. Quartier, B. Buchmann, and L. Emmenegger (2008), Determination of biogenic and fossil CO_2 emitted by waste incineration based on (CO_2)-C-14 and mass balances, *Bioresour. Technol.*, *99*(14), 6471–6479, doi:10.1016/j.biortech.2007.11.042.

Mohr, C., et al. (2012), Identification and quantification of organic aerosol from cooking and other sources in Barcelona using aerosol mass spectrometer data, *Atmos. Chem. Phys.*, *12*, 1649–1665, doi:10.5194/acp-12-1649-2012.

National Institute for Occupational Safety and Health (1999), Elemental carbon (diesel particulate): Method 5040, Rep. [Available at www.cdc.gov./niosh/nmam/pdfs/5040f3.pdf.]

Orasche, J., J. Schnelle-Kreis, G. Abbaszade, and R. Zimmermann (2011), Technical Note: In-situ derivatization thermal desorption GC-TOFMS for direct analysis of particle-bound non-polar and polar organic species, *Atmos. Chem. Phys.*, *11*(17), 8977–8993, doi:10.5194/acp-11-8977-2011.

Paatero, P., and U. Tapper (1994), Positive Matrix Factorization: A nonnegative factor model with optimal utilization of error-estimates of data values, *Environmetrics*, *5*(2), 111–126, doi:10.1002/env.3170050203.

Peterson, M. R., and M. H. Richards (2002), Thermal-optical-transmittance analysis for organic, elemental, carbonate, total carbon, and OCX2 in PM2.5 by the EPA/NIOSH method, Pittsburgh.

Piazzalunga, A., V. Bernardoni, P. Fermo, G. Valli, and R. Vecchi (2011), Technical Note: On the effect of water-soluble compounds removal on EC quantification by TOT analysis in urban aerosol samples, *Atmos. Chem. Phys.*, *11*(19), 10,193–10,203, doi:10.5194/acp-11-10193-2011.

Platt, S. M., et al. (2013), Secondary organic aerosol formation from gasoline vehicle emissions in a new mobile environmental reaction chamber, *Atmos. Chem. Phys.*, *13*(18), 9141–9158, doi:10.5194/acp-13-9141-2013.

Pollack, I. B., et al. (2012), Airborne and ground-based observations of a weekend effect in ozone, precursors, and oxidation products in the California South Coast Air Basin, *J. Geophys. Res.*, *117*, D00V05, doi:10.1029/2011JD016772.

Pope, C. A., and D. W. Dockery (2006), Health effects of fine particulate air pollution: Lines that connect, *J. Air Waste Manage. Assoc.*, *56*(6), 709–742, doi:10.1080/10473289.2006.10464485.

Pöschl, U. (2005), Atmospheric aerosols: Composition, transformation, climate and health effects, *Angew. Chem., Int. Ed.*, *44*(46), 7520–7540, doi:10.1002/anie.200501122.

Putaud, J.-P., et al. (2004), A European aerosol phenomenology-2: Chemical characteristics of particulate matter at kerbside, urban, rural and background sites in Europe, *Atmos. Environ.*, *38*(16), 2579–2595, doi:10.1016/j.atmosenv.2004.01.041.

Robinson, A. L., R. Subramanian, N. M. Donahue, A. Bernardo-Bricker, and W. F. Rogge (2006), Source apportionment of molecular markers and organic aerosols-1. Polycyclic aromatic hydrocarbons and methodology for data visualization, *Environ. Sci. Technol.*, *40*(24), 7803–7810, doi:10.1021/es0510414.

Ruff, M., L. Wacker, H. W. Gaggeler, M. Suter, H. A. Synal, and S. Szidat (2007), A gas ion source for radiocarbon measurements at 200 kV, *Radiocarbon*, *49*(2), 307–314, doi:10.2458/azu_js_rc.v.2930.

Ruff, M., S. Szidat, H. W. Gäggeler, M. Suter, H. A. Synal, and L. Wacker (2010), Gaseous radiocarbon measurements of small samples, *Nucl. Instrum. Methods Phys. Res., Sect. B*, *268*(7–8), 790–794, doi:10.1016/j.nimb.2009.10.032.

Sandradewi, J., et al. (2008), Comparison of several wood smoke markers and source apportionment methods for wood burning particulate mass, *Atmos. Chem. Phys. Discuss.*, *8*(2), 8091–8118, doi:10.5194/acpd-8-8091-2008.

Schauer, J. J., W. F. Rogge, L. M. Hildemann, M. A. Mazurek, G. R. Cass, and B. R. T. Simoneit (1996), Source apportionment of airborne particulate matter using organic compounds as tracers, *Atmos. Environ.*, *30*(22), 3837–3855, doi:10.1016/1352-2310(96)00085-4.

Schauer, J. J., M. J. Kleeman, G. R. Cass, and B. R. T. Simoneit (2002a), Measurement of emissions from air pollution sources. 4. C-1-C-27 organic compounds from cooking with seed oils, *Environ. Sci. Technol.*, *36*(4), 567–575, doi:10.1021/es002053m.

Schauer, J. J., M. J. Kleeman, G. R. Cass, and B. R. T. Simoneit (2002b), Measurement of emissions from air pollution sources. 5. C-1-C-32 organic compounds from gasoline-powered motor vehicles, *Environ. Sci. Technol.*, *36*(6), 1169–1180, doi:10.1021/es0108077.

Schmid, H., et al. (2001), Results of the "carbon conference" international aerosol carbon round robin test stage I, *Atmos. Environ.*, *35*(12), 2111–2121.

Schnelle-Kreis, E., M. Sklorz, A. Peters, J. Cyrys, and R. Zimmermann (2005), Analysis of particle-associated semi-volatile aromatic and aliphatic hydrocarbons in urban particulate matter on a daily basis, *Atmos. Environ.*, *39*(40), 7702–7714, doi:10.1016/j.atmosenv.2005.04.001.

Slowik, J. G., et al. (2010), Characterization of a large biogenic secondary organic aerosol event from eastern Canadian forests, *Atmos. Chem. Phys.*, *10*(6), 2825–2845, doi:10.5194/acp-10-2825-2010.

Stuiver, M., and H. A. Polach (1977), Reporting of C-14 data—Discussion, *Radiocarbon*, *19*(3), 355–363, doi:10.2458/azu_js_rc.v.493.

Subramanian, R., N. M. Donahue, A. Bernardo-Bricker, W. F. Rogge, and A. L. Robinson (2006), Contribution of motor vehicle emissions to organic carbon and fine particle mass in Pittsburgh, Pennsylvania: Effects of varying source profiles and seasonal trends in ambient marker concentrations, *Atmos. Environ.*, *40*(40), 8002–8019, doi:10.1016/j.atmosenv.2006.06.055.

Sun, Y. L., et al. (2011), Characterization of the sources and processes of organic and inorganic aerosols in New York city with a high-resolution time-of-flight aerosol mass spectrometer, *Atmos. Chem. Phys.*, *11*(4), 1581–1602, doi:10.5194/acp-11-1581-2011.

Synal, H.-A., M. Stocker, and M. Suter (2007), MICADAS: A new compact radiocarbon AMS system, *Nucl. Instrum. Methods Phys. Res., Sect. B*, *259*(1), 7–13, doi:10.1016/j.nimb.2007.01.138.

Szidat, S. (2009), Sources of Asian haze, *Science*, *323*(5913), 470–471, doi:10.1126/science.1169407.

Szidat, S., et al. (2004a), Radiocarbon (^{14}C)-deduced biogenic and anthropogenic contributions to organic carbon (OC) of urban aerosols from Zürich, Switzerland, *Atmos. Environ.*, *38*(24), 4035–4044, doi:10.1016/j.atmosenv.2004.03.066.

Szidat, S., T. M. Jenk, H. W. Gäggeler, H. A. Synal, I. Hajdas, G. Bonani, and M. Saurer (2004b), THEODORE, a two-step heating system for the EC/OC determination of radiocarbon (^{14}C) in the environment, *Nucl. Instrum. Methods Phys. Res., Sect. B*, *223–224*, 829–836, doi:10.1016/j.nimb.2004.04.153.

Szidat, S., T. M. Jenk, H. A. Synal, M. Kalberer, L. Wacker, I. Hajdas, A. Kasper-Giebl, and U. Baltensperger (2006), Contributions of fossil fuel, biomass-burning, and biogenic emissions to carbonaceous aerosols in Zurich as traced by C-14, *J. Geophys. Res.*, *111*, D07206, doi:10.1029/2005JD006590.

Szidat, S., A. S. H. Prévôt, J. Sandradewi, M. R. Alfarra, H.-A. Synal, L. Wacker, and U. Baltensperger (2007), Dominant impact of residential wood burning on particulate matter in Alpine valleys during winter, *Geophys. Res. Lett.*, *34*, L05820, doi:10.1029/2006GL028325.

Szidat, S., M. Ruff, N. Perron, L. Wacker, H. A. Synal, M. Hallquist, A. S. Shannigrahi, K. E. Yttri, C. Dye, and D. Simpson (2009), Fossil and non-fossil sources of organic carbon (OC) and elemental carbon (EC) in Goteborg, Sweden, *Atmos. Chem. Phys.*, *9*(5), 1521–1535, doi:10.5194/acp-9-1805-2009.

Szidat, S., et al. (2013), Intercomparison of C-14 analysis of carbonaceous aerosols: Exercise 2009, *Radiocarbon*, *55*(2–3), 1496–1509, doi:10.2458/azu_js_rc.55.16314.

Thompson, J. E., P. L. Hayes, J. L. Jimenez, K. Adachi, X. Zhang, J. Liu, R. J. Weber, and P. R. Buseck (2012), Aerosol optical properties at Pasadena, CA during CalNex 2010, *Atmos. Environ.*, *55*, 190–200, doi:10.1016/j.atmosenv.2012.03.011.

Ulbrich, I. M., M. R. Canagaratna, Q. Zhang, D. R. Worsnop, and J. L. Jimenez (2009), Interpretation of organic components from positive matrix factorization of aerosol mass spectrometric data, *Atmos. Chem. Phys.*, *9*(9), 2891–2918, doi:10.5194/acp-9-2891-2009.

Viana, M., X. Chi, W. Maenhaut, J. Cafmeyer, X. Querol, A. Alastuey, P. Mikuška, and Z. Večeřa (2006), Influence of sampling artefacts on measured PM, OC, and EC levels in carbonaceous aerosols in an urban area, *Aerosol Sci. Technol.*, *40*(2), 107–117, doi:10.1080/02786820500484388.

Wacker, L., M. Christl, and H. A. Synal (2010), Bats: A new tool for AMS data reduction, *Nucl. Instrum. Methods Phys. Res., Sect. B*, *268*(7–8), 976–979, doi:10.1016/j.nimb.2009.10.078.

Wacker, L., S. M. Fahrni, I. Hajdas, M. Molnar, H. A. Synal, S. Szidat, and Y. L. Zhang (2013), A versatile gas interface for routine radiocarbon analysis with a gas ion source, *Nucl. Instrum. Methods Phys. Res., Sect. B*, *294*, 315–319, doi:10.1016/j.nimb.2012.02.009.

Wagner, N. L., et al. (2012), The sea breeze/land breeze circulation in Los Angeles and its influence on nitryl chloride production in this region, *J. Geophys. Res.*, *117*, D00V24, doi:10.1029/2012JD017810.

Washenfelder, R. A., et al. (2011), The glyoxal budget and its contribution to organic aerosol for Los Angeles, California, during CalNex 2010, *J. Geophys. Res.*, *116*, D00V02, doi:10.1029/2011JD016314.

Williams, B. J., A. H. Goldstein, N. M. Kreisberg, S. V. Hering, D. R. Worsnop, I. M. Ulbrich, K. S. Docherty, and J. L. Jimenez (2010), Major components of atmospheric organic aerosol in southern California as determined by hourly measurements of source marker compounds, *Atmos. Chem. Phys.*, *10*(23), 11,577–11,603, doi:10.5194/acp-10-11577-2010.

Wonaschutz, A., S. P. Hersey, A. Sorooshian, J. S. Craven, A. R. Metcalf, R. C. Flagan, and J. H. Seinfeld (2011), Impact of a large wildfire on water-soluble organic aerosol in a major urban area: The 2009 Station Fire in Los Angeles County, *Atmos. Chem. Phys.*, *11*(16), 8257–8270, doi:10.5194/acp-11-8257-2011.

World Health Organization (2006), Air quality guidelines for particulate matter, ozone, nitrogen dioxide and sulfur dioxide. Global update 2005. Summary of risk assessment, document WHO/SDE/PHE/OEH/06.02, World Health Organization, Geneva.

Zapf, A., A. Nesje, S. Szidat, L. Wacker, and M. Schwikowski (2013), C-14 measurements of ice samples from the Juvfonne ice tunnel, Jotunheimen, southern Norway-validation of a C-14 dating technique for glacier ice, *Radiocarbon*, *55*(2–3), 571–578, doi:10.2458/azu_js_rc.55.16320.

Zhang, Y. L., N. Perron, V. G. Ciobanu, P. Zotter, M. C. Minguillón, L. Wacker, A. S. H. Prévôt, U. Baltensperger, and S. Szidat (2012), On the isolation of OC and EC and the optimal strategy of radiocarbon-based source apportionment of carbonaceous aerosols, *Atmos. Chem. Phys.*, *12*(22), 10,841–10,856, doi:10.5194/acp-12-10841-2012.